Experimental evaluation of the optimal position of a macroencapsulated phase change material incorporated composite roof under hot climate conditions

Qudama Al-Yasiri [a,b,c,*], Márta Szabó [b]

[a] *Mechanical Engineering Doctoral School, Szent István University, Páter K. u. 1, Gödöllő H-2100, Hungary*
[b] *Department of Building Services and Environmental Engineering, Faculty of Mechanical Engineering, Szent István University, Páter K. u. 1, Gödöllő H-2100, Hungary*
[c] *Department of Mechanical Engineering, Faculty of Engineering, University of Misan, Al Amarah City, Maysan Province 62001, Iraq*

ARTICLE INFO

ABSTRACT

This paper experimentally investigates the optimal position of a phase change material (PCM) incorporated composite roof under Iraq climatic conditions. The roof composed of Isogam (4 mm), concrete (50 mm) and gypsum board (8 mm) which is an Iraqi popular roof combination. Four models are installed and tested; one represented the reference roof (Model A) and the others incorporated with PCM. The PCM placed between Isogam and concrete (Model B), in the middle of concrete (Model C), and between the concrete and gypsum board (Model D). Set of indicators are introduced to compare among models considering the test room temperature, outside and inside roof surface temperatures. These indicators are the room maximum temperature reduction (RMTR), average temperature fluctuation reduction (ATFR), decrement factor (DF), time lag (TL) and heat flux reduction (HFR). Results showed that Model B verified the best thermal performance, and the PCM was effectively working at high outside temperatures. The maximum room temperature of PCM models was reduced by up to 9 °C compared with the reference model. Moreover, a maximum of 12.9%, 8.4–9.5 °C, 0.44–0.49, 140–180 min, 47.9–64.6% of respectively RMTR, ATFR, DF, TL, and HFR, are obtained for Model B under high outside temperatures.

Introduction

Buildings and constructions are responsible for more than 36% of global final energy end-use and 39% of CO_2 emissions due to rapid population and urbanisation [1]. Therefore, serious improvements towards sustainable buildings are required to meet the Paris Agreement's target by improving buildings' energy intensity by up to 30% by 2030 compared with 2015 [2]. Amongst recent technologies, building envelope based PCM is a booming technology nowadays that showed remarkable benefits concerning building energy efficiency through improving the building thermal comfort and energy saving [3–6]. Despite the remarkable advances of PCMs to improve the thermal performance of any envelope element integrated with, there are still open questions regarding key parameters for their efficient use, such as PCM's influential position. PCM's best position within the building envelope plays a predominant role in controlling the PCM performance, which depends highly on the PCM thermal properties and environmental conditions [7]. In other words, specifying PCM's optimal position within the building envelope is a key factor of the technology. It affects the rate and time to reach the full exploitation of PCM potential, influencing the building's energy performance accordingly [8].

Researchers have made efforts to point out the PCM layer's optimal position under different climatic conditions, but no universal agreement has been reached. Under hot locations, studies were chiefly concluded three influential positions, namely close to the envelope exterior, middle of the envelope and, close to the indoor environment. Lagou et al. [9] numerically investigated PCM's optimal position integrated non-conditioned buildings in diverse European countries at different locations. Analytical results revealed that the PCM should be placed in the interior edge to get the best PCM performance for all locations, including the hot ones. Hu and Yu [10] numerically studied the optimal position concerning the insulation in roof combination in five cities of China. Under summer conditions, the results showed that the optimal PCM position is to the inside of insulation where the cooling loads were decreased remarkably. The reason attributed to that the heat transferred

from the outdoor to the indoor was minimised due to roof layers thermal resistance, and only little amount was passed and stored into the PCM layer. Hagenau and Jradi [11] numerically studied the optimal position of PCMs having different melting temperatures under Danish climatic conditions, placed at three positions (between the interior gypsum and insulation layers, between the insulation and concrete layer, and to the outdoor environment). PCMs with a melting temperature of 24 °C (CrodaTherm24, RT24, SP24E) resulted in the best thermal performance, especially when placed between the interior gypsum and insulation layers. They concluded that an energy saving of 7–15% was obtained along with a reduction of 4 °C in the average summer indoor air temperature. Besides, Tunçbilek et al. [12] numerically studied different positions of PCMs incorporated office walls under intermittent cooling load. They stated that positioning the PCM near the interior can save energy by 12.8%, considering the optimal phase change temperature (25 °C) and optimal thickness. Moreover, the study concluded that placing PCM near the exterior position has a negative energy saving and increases the cooling loads. This is because that exterior position required higher PCM melting temperatures (above 25 °C) to be implemented for better energy-saving.

In other studies, placing the PCM layer at the middle position improves the energy-saving by up to 75%, especially at high solar radiation locations [13]. Triano-Juárez et al. [14] numerically studied three PCM positions (near the inner surface, middle position and near to the outer surface) of a concrete roof under Mexico's warm climate conditions. The results showed a negligible difference in changing PCM position. However, the middle position showed the maximum energy saving compared with the standard roof without PCM. Beside, Dashtaki et al. [15] numerically studied the best position of different PCM types embedded into a composite wall under weather conditions of Tehran, Iran. Findings indicated that the middle position of PCM layer has the best thermal performance in terms of heat transfer rate reduction.

On the contrary, several researchers have stated that the outside position is the best for PCM incorporated buildings under hot and warm conditions. Arici et al. [16] numerically studied the optimum position of a PCM layer with different thicknesses and melting temperatures for three cities in Turkey. They concluded that placing the PCM between the insulation and outer envelope layer provides higher energy saving under hot conditions. Saadi and Daouas [17] numerically analysed the PCM layer's best position under Tunisian weather conditions. Authors stated that the outdoor position is the best considering the reduced cooling loads and saved energy. Moreover, they concluded that PCM incorporation is cost-effective when integrated with building envelopes with no insulation. Li et al. [18] also numerically studied different PCM types

considering the PCM layer's repositioning near the indoor environment, near the outdoor environment and middle position. In all studied cases, the outdoor environment position showed the PCM layer's best performance, where the highest heat transfer reduction was obtained due to the melting of PCM. Heim and Wieprzkowicz [19] investigated the effect of PCM layer repositioning on a lightweight construction's annual thermal insulation, considering the temperature of internal and external environments in central Europe. The PCM layer placed at five different positions varies between the internal and external environments. Their numerical results showed that the external position was the best in terms of the temperature stability inside the insulation and the minimised temperature fluctuation. Yu et al. [20] studied different PCM types for different China locations, making a comparison based on placing the PCM at the outer position. Despite the best PCM type for each location, results indicated that the outer position is effective for hot summer locations. The decrement factor and peak inner surface temperature were reduced respectively by 85.78% and 3.9 °C in the hot summer-cold winter locations. The maximum reduction of these indicators was 87.83% and 3.8 °C for hot summer-warm winter locations.

In this study, incorporation of PCM within a composite flat roof was examined as an effective passive strategy to decrease the cooling loads and save energy in buildings under hot locations. This strategy has little attention for roofs than walls, although the roofs are exposed to solar radiation longer period (flat roofs in particular). The PCM layer's optimal position was experimentally examined for non-conditioned models based on popular composite roof combination materials. Three influential positions for the PCM layer have been studied, namely between the finishing and main roof layers, at the middle of the main roof layer, and between the main and cladding layers. Models were subjected to actual hot weather conditions of Al Amarah city, Iraq under two cases: Case I (when the standard finishing layer used) and Case II (when the finishing layer gains more heat). Consequently, several indicators considering reducing room temperature and inside surface temperature against the average outside surface temperature have been studied to reach a fair evaluation for the studied positions.

Materials and methods

Experimental models

The experiments have been conducted along seven days during August and September 2020 starting from 6:00 a.m. under hot climatic weather conditions of Al Amarah city (Latitude: 31.84° & Longitude: 47.14°), Maysan province, Iraq. Four identical test rooms were

fabricated in the experiment, mainly are (i) Model A: a reference room consists of the three traditional layers (finishing layer - main layer - cladding layer), (ii) Model B: a room contains additional PCM layer placed between the finishing layer and the main layer, (iii) Model C: a room contains PCM placed in the middle of the main layer and, (iv) Model D: a room where the PCM layer placed between the main layer and cladding layer (shown in Fig. 1). Two cases were investigated in this work in which how the finishing layer affects the absorptivity of a composite roof and results in higher outside surface temperatures.

As this work focuses on the roof, high-density cork boxes were considered as the floor and sidewalls of tested models. The boxes have a thickness (L) of 30 mm and have length, width and height of 40*30*23 cm, respectively. Boxes are locally available and often used for ice-cream storing and low-temperature foods preservation due to their high thermal insulation behaviour. The boxes are covered with a high-quality fiberglass insulator (L = 20 mm, thermal conductivity (k) = 0.043 W/m.K) for further insulation to guarantee that the heat passes through the roof layers only.

The roof of each model was comprised of three layers, namely are Isogam layer (L = 4 mm, k = 0.24 W/m.K), concrete layer (L = 50 mm, k = 1.49 W/m.K) and gypsum mortar layer (L = 8 mm, k = 0.36 W/m.K). This roof combination is a popular roof combination installed in residential buildings in the city, with the worst thermal behaviour and high cooling loads [21]. It is worth mentioning that all layers were smoothed to make sure of perfect contact between each two. Every layer has been sealed separately using high-quality insulation foam during the installation. The foam is essential to guarantee no air infiltration from outside towards the test room, and vice versa and heat would be exchanged only through the roof layers. A detailed description of composite roof layers is shown in Table 1.

PCM

Under hot climate conditions, the PCM used to restrict the heat transferred from outdoor towards indoor, which works as a heat barrier to reduce the cooling loads through shaving and shifting peak temperatures. In this regard, PCMs of high melting temperatures are

recommended to guarantee suitable heat storage potential. Selection of the appropriate PCM candidate, is essential considering two concerns: (i) the PCM does not melt quickly during the beginning of the day, and (ii) the night cooling effect should be considered to repeat the cycle passively for the next day. For those reasons, paraffin wax (44 °C melting temperature) was selected in this work due to its suitability for temperature variation in the studied location as well as its availability with low cost in the market, safe operation, compatibility with a wide range of encapsulation materials and other desired properties [23]. Paraffin wax used in this work is popular in Iraq as it produced from the Iraqi refineries during the dewaxing process and investigated in several studies for different applications [24–26]. The thermophysical properties of this PCM are listed in Table 2.

Generally, PCMs are suffering from low thermal conductivity which impacts their melting and solidification time. Therefore, several enhancement methods were proposed to improve it, such as the dispersion of nanoparticles, metallic foam insertion, and high thermal conductivity macroencapsulation containers [28]. In this work, the PCM was macroencapsulated inside panels (L = 1 cm) made from galvanised steel sheet (L = 0.4 mm). This metal sheet was carefully chosen due to its high thermal conductivity, locally available with low price, easy to be formed and welded and, compatible with the construction materials and paraffin [29,30]. A quantity of 0.5 kg of paraffin wax was weighted using a precise electronic scale, melted by a gas boiler, and poured inside each panel. This quantity is appropriate to guarantee no leakage during the melting phase that may result from the volumetric change or inclined roof layers during installation. The main steps followed to prepare the PCM panels are shown in Fig. 3.

Measurement devices

In this work, data logger contains fifteen thermocouples of T-type (0.2 mm, ± 1 °C accuracy and ± 0.5 °C limits of error) installed at different positions of the roof layers (on the outer surface of finishing layer, beneath PCM layer, beneath the cladding layer and inside the test room), as shown in Fig. 1. The thermocouples were connected to multichannel Arduino (type Mega 2560) provided by Ardunic Sinaa, Baghdad

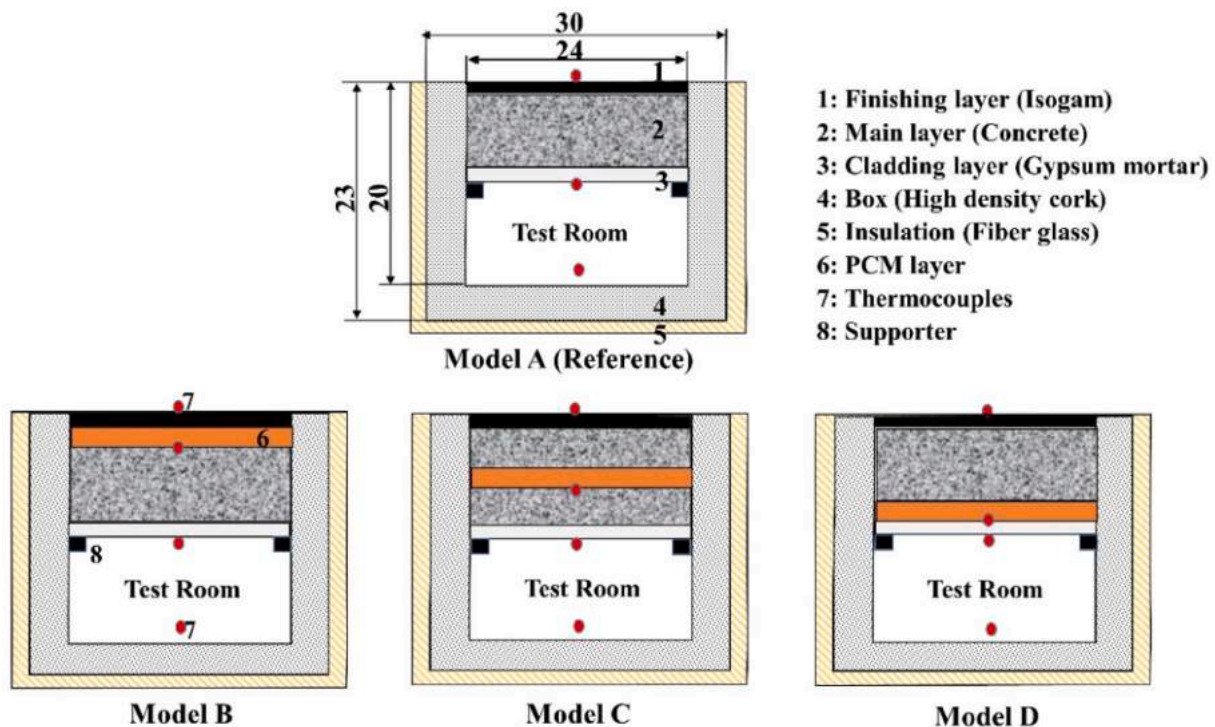

1: Finishing layer (Isogam)
2: Main layer (Concrete)
3: Cladding layer (Gypsum mortar)
4: Box (High density cork)
5: Insulation (Fiber glass)
6: PCM layer
7: Thermocouples
8: Supporter

Fig. 1. Schematic view of the proposed models.

Fig. 2. Fabricating of concrete layers.

Table 1
Description of roof layers used in the experimental work.

Roof layer	Description
Isogam (finishing layer)	Local roofing and waterproof material increasingly used in the last 15 years in Iraq as an alternative to the concrete tiles and other traditional roofing materials [21]. It is mainly made from bitumen-rubber mastic and laminated from both sides with a thin plastic layer (one of them coated with silver colour to reflect the solar radiation). This plastic layer is removable and highly influenced by changeable weather conditions which limiting its reflectivity. In this study, Isogam has installed in two cases: Case I, in which a regular Isogam used, and Case II, when removing the reflecting layer. The latter case allows high heat to be transferred towards the test room, which is essential in this work to investigate PCM's potential at a high range of temperatures.
Concrete (main layer)	Concrete layers were fabricated according to the concrete mix ratio 1:2:3 of raw materials (cement: sand: gravel) used for residential building roofs in Iraq, which has c25-30 Mpa [22]. Locally used raw materials (i.e., cement, sand and gravel) were mixed with water to fabricate the concrete mixture. The mixture was poured into moulds and left dried naturally. Fig. 2, shows the procedure followed to prepare the concrete layers.
Gypsum mortar (cladding layer)	Locally available pre-fabricated gypsum boards were used in this work. These boards are made from gypsum (L = 6 mm), covered by thin carton sheets (1 mm) from both sides. These boards are popularly used for suspended ceiling installations. They have been used in the current work as they have adequate strength to carry the heavy-weight concrete layer and contain gypsum used for cladding in the Iraqi buildings.

Table 2
Thermo-physical properties of used PCM [27].

Thermal conductivity (W/m.K)	Density (kg/m^3)	Latent heat of fusion (kJ/kg)	Specific heat (KJ/kg.K)
0.21	930 (solid) 830 (liquid)	190	2.1 (solid) 2.1 (liquid)

Evaluation of thermal performance

Several indicators have been discussed to evaluate the benefits earned from PCM incorporation into Model B, Model C and Model D compared with Model A, which designate the PCM layer's optimal position. These indicators are (i) room maximum temperature reduction, (ii) average temperature fluctuation reduction, (iii) decrement factor, (iv) time lag and, (v) heat flux reduction. Average outside roof surface temperature (T_o), inside surface temperature (T_i) and room temperature (T_r) for each model, were used to identify the above indicators.

Results and discussion

As mentioned previously, the experimental work lasted for seven days during August and September 2020. They are among the hottest months in summer (in addition to July) wherein the country exposed to high temperature and solar radiation (SR), as shown in Fig. 5. The measurements of Case I lasted for three consecutive days (29-31.08.2020), whereas Case II lasted for four consecutive days (11–14.09.2020) to investigate the effect of high temperatures for a longer time.

Fig. 6 and Fig. 7 show the variation of temperatures (T_o, T_i, T_r and T_{PCM}) as a function of time for Model A, Model B, Model C and Model D, respectively in case I and case II experiments. As expected, it can be noticed that all models containing PCM layer have better thermal performance than the reference case thanks to the thermal storage potential of the PCM layer. The maximum value of T_o reached 60.8 °C, 59.3 °C and 58.2 °C in the first, second and third cycle of Case I. Whereas, T_o reached

[31]. The data logger is programmed to record temperatures every 10 min (time step) and save them into 4 GB storage memory. The solar radiation was collected manually every 30 min during the experimental days using a solar power meter (Model SM206) with 0.1 W/m^2 resolution and 10 W/m^2 accuracy. Models and measuring devices are shown in Fig. 4.
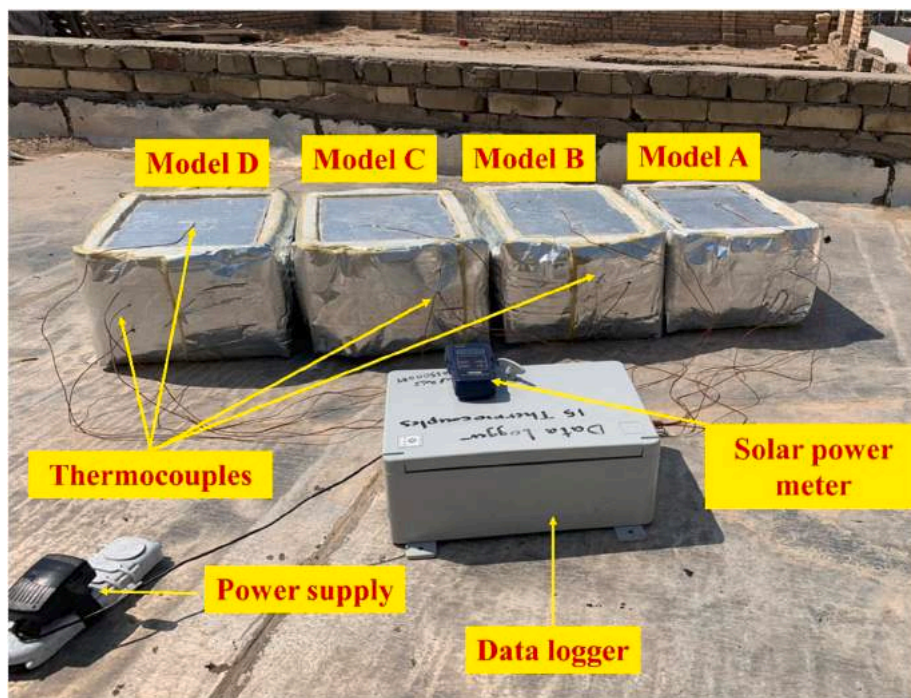
Fig. 3. Preparation of the PCM panel.

Fig. 4. Experimental models.

a maximum of 76.4 °C, 75.4 °C, 75.5 °C and 73.25 °C respectively in the first, second, third and fourth cycle of Case II. Peak temperatures were reached in the midday from 12:30 to 13:00 in both cases in conjunction with the highest solar radiation.

By making a quick comparison among Case I and Case II figures considering the difference between T_o and T_r, we can recognise that PCM is working better at higher T_o. It is attributed to the high melting temperature of used PCM, which requires more heat to be utilised sufficiently.

Several indicators are discussed to evaluate the best thermal performance amongst Model B, Model C and Model D resulted from PCM optimal position compared with Model A, as follows:

Room maximum temperature reduction (RMTR)

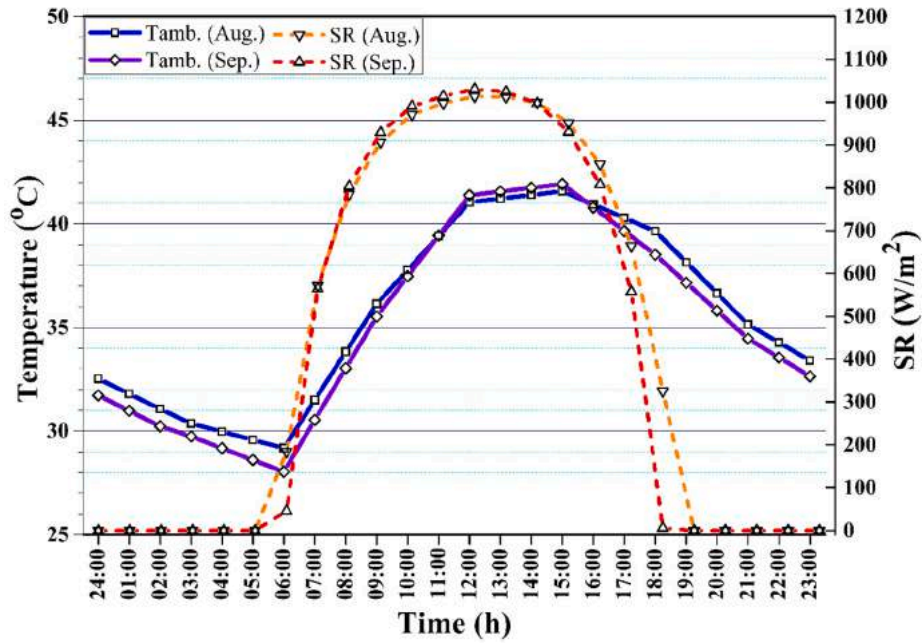PCMs can remarkably reduce indoor temperatures thanks to their

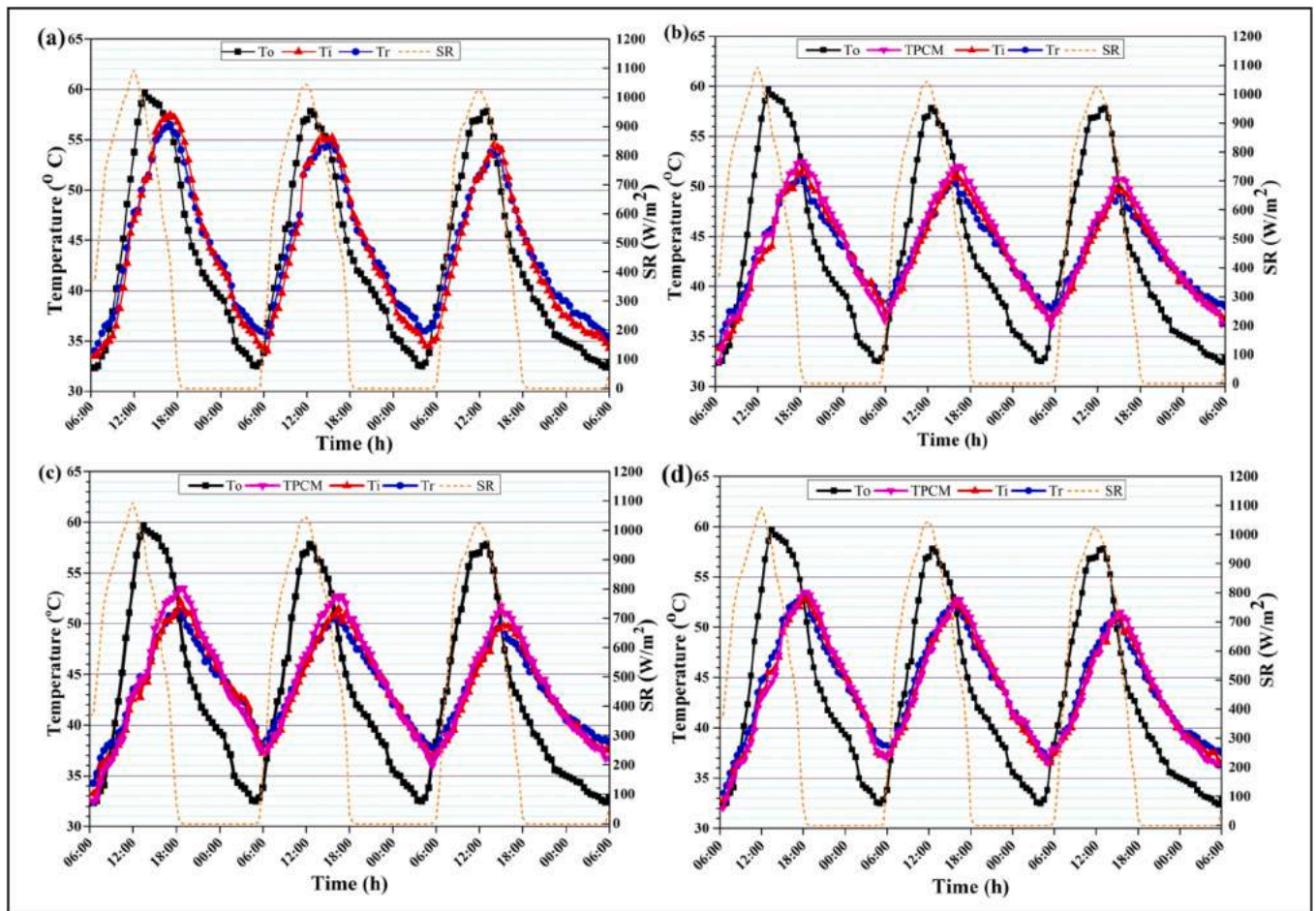**Fig. 5.** Hourly average ambient temperature and solar radiation during August and September [32].

Fig. 6. Temperature profile of Case I: (a) Model A; (b) Model B; (c) Model C; (d) Model D.
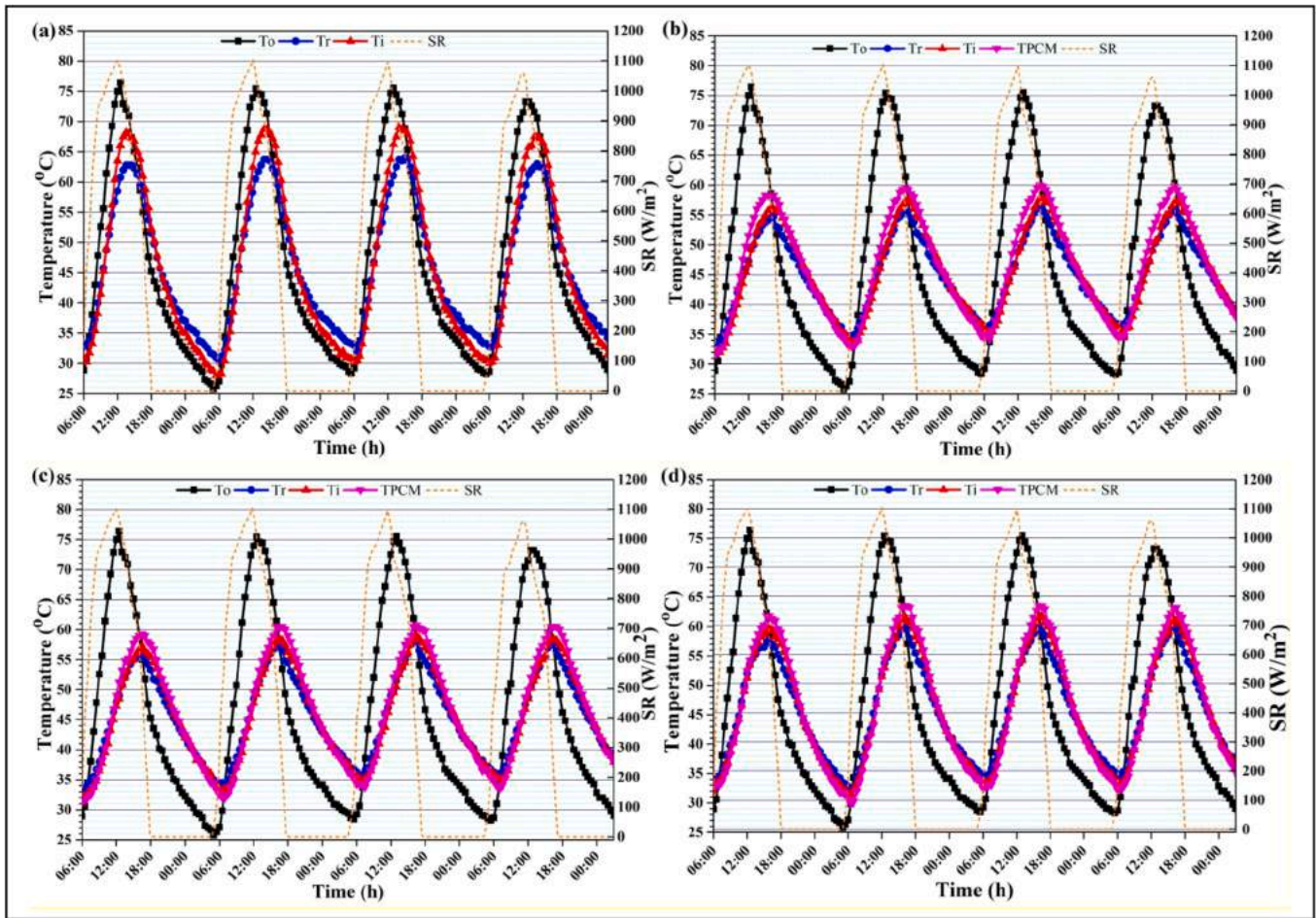
Fig. 7. Temperature profile of Case II: (a) Model A; (b) Model B; (c) Model C; (d) Model D.
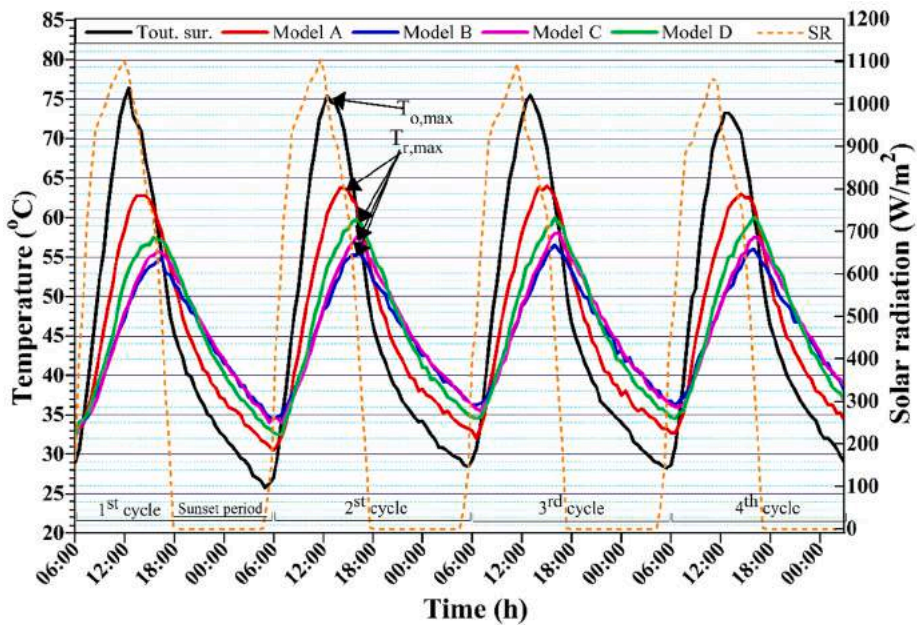
Fig. 8. Curves of T_r for test models (Case II).

thermal energy storage. This can be observed by comparing T_r for all models. For instance, the maximum T_r recorded for Model A, Model B, Model C and Model D in the first cycle of Case II (shown in Fig. 8) are

respectively 62.75 °C, 54.75 °C, 55.75 °C and 57.5 °C against T_o equal to 76.4 °C. Those values represent a reduction of 9 °C, 8 °C and 5.25 °C in the T_r of Model B, Model C and Model D compared with Model A.

RMTR shows how high the reduction in T_r inside the test room is due to incorporating the PCM layer, which impacts the cooling and air-conditioning systems' reliance on real-scale cases. RMTR can be presented in terms of the maximum T_o and maximum T_r for PCM rooms compared to the reference room (i.e., without PCM layer). RMTR was calculated using Eq. (1), in which higher RMTR means better heat shaving through the roof, as follows:

$$RMTR = \frac{T_{r,max.ref.} - T_{r,max.PCM}}{T_{r,max.ref.}} \times 100\% \quad (1)$$

where $T_{r,max.ref.}$ and $T_{r,max.PCM}$ are the maximum temperature of T_r for Model A and PCM models, respectively. The calculated RMTR in Case I and Case II are shown in Fig. 9.

As clarified in Fig. 9, Model B showed the best thermal performance in all cycles. Furthermore, Model B at higher temperature case (i.e., Case II) performed better than lower temperature case, which shows higher utilisation of PCM storage capacity. On the other hand, Model D shows the worst performance amongst other PCM models in RMTR. This indicates the PCM layer's negative effect when placed near the interior of the non-conditioned environment under hot climates. The highest RMTR obtained by Model B, Model C and Model D in Case I was 10.3%, 8.1% and 5.1% higher than Model A at the maximum T_o of 60.8 °C and 58.2 °C (first and third cycles), respectively. Likewise, the highest RMTR in Case II reached 12.9%, 11.2% and 8.4% at the maximum T_o in the first and second cycles (i.e., 76.4 °C and 75.4 °C, respectively) for PCM models compared with the referenced model.

Average temperature fluctuation reduction (ATFR)

This indicator represents the average decrement of test room temperature fluctuation during the day and night period. It is calculated by combining the average decrease of room temperature in the day "X" with the average increase of room temperature in the night period "Y" according to Eq. (2) - Eq. (4), as follows [33]:

$$ATFR = X + Y \quad (2)$$

$$X = T_{r,av.,ref.} - T_{r,av.,PCM} \quad (3)$$

$$Y = T_{r,av.,PCM} - T_{r,av.,ref.} \quad (4)$$

where $T_{r\,av.,ref.}$ is the average temperature of the reference room (Model A), and $T_{r\,av.,PCM}$ is the average temperature of the room containing PCM (i.e., Model B, Model C and Model D) (°C). AFTR is calculated considering the time 6:00–18:00 to calculate X, and the time 18:00–6:00 to calculate the value of Y in each day-cycle. ATFR of Case I and Case II cycles is represented in Fig. 10.

This indicator has to be more than 1 °C to indicate PCM potential utilisation in the building envelope [33]. Generally, all positions of PCM models have effectively restrained the fluctuations of room temperature. Here, it can be noticed that Model C showed the best behaviour even better than Model B, and then, Model D.

It is also noted that the PCM layer at all positions had a better thermal performance at high T_o which means that more heat was stored into the PCM which damping temperature fluctuations. On average, the ATFR was reduced by 6.1–6.8 °C in Model B, 7.1–7.7 °C in Model C, and by 4.8 °C-5.9 °C in Model D for Case I. Moreover, the value of ATFR ranged between 8.4 and 9.5 °C, 8.5–9.3 °C, 6.2–6.4 °C for Model B, Model C and Model D, respectively for the Case II. Latter values indicated the advantage of using PCM under hot climates which is much higher than those obtained in the literature [33–35]. For instance, highest values of ATFR ranged between 3 and 4 °C were obtained in a study conducted under Australian conditions [36], which reflects the suitability of used PCM in the current work for the Iraqi solar radiation which effectively exploited the heat storage potential of selected PCM.

As long as ATFR deals with room temperature at day and night periods, it is important to study PCM's thermal behaviour during melting and solidification phases. As shown in Fig. 11, it can be appreciated that the PCM temperature of Model B is higher than the temperature of other models in the first half of the day in each cycle. It is attributed to that PCM layer in Model B is placed close to the exterior environment and restricting the high solar radiation during the early hours of the day, and the heat was charged into the PCM before other models. For Model D, the PCM temperature was high at the beginning of the day influenced by room high temperature as the thermocouple placed beneath the PCM layer and close to the test room. The PCM temperature of Model C was in between the two models most of the time, which showed more stable room temperatures during the day and night periods and resulted in better ATFR.

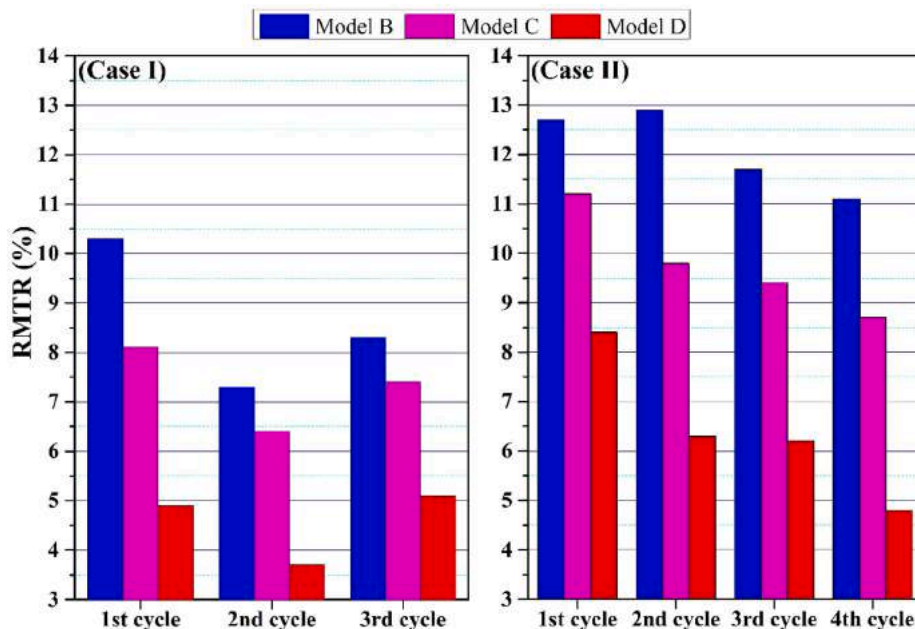For solidification phase, the PCM temperature of Model B was

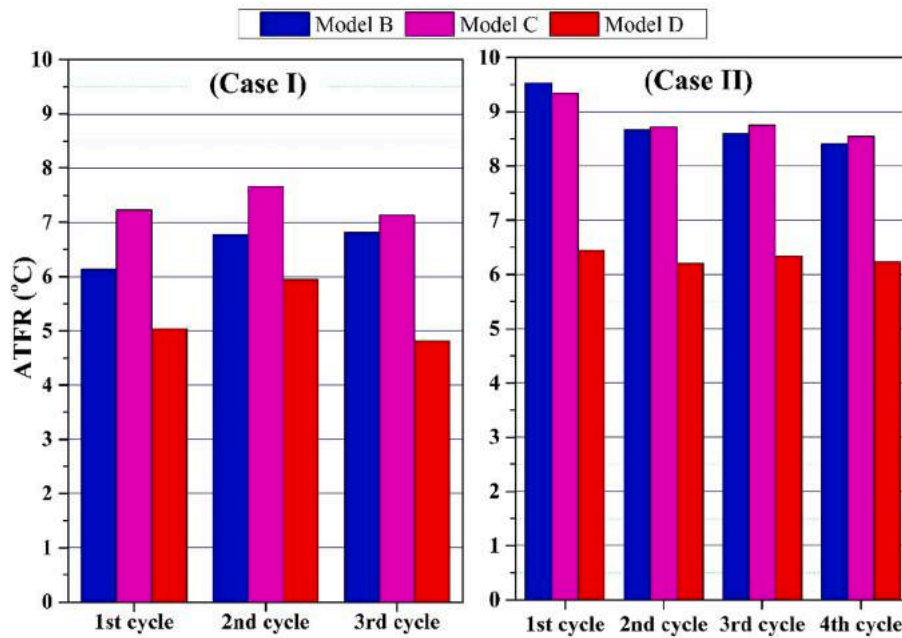**Fig. 9.** RMTR during peak hours for Case I and Case II.
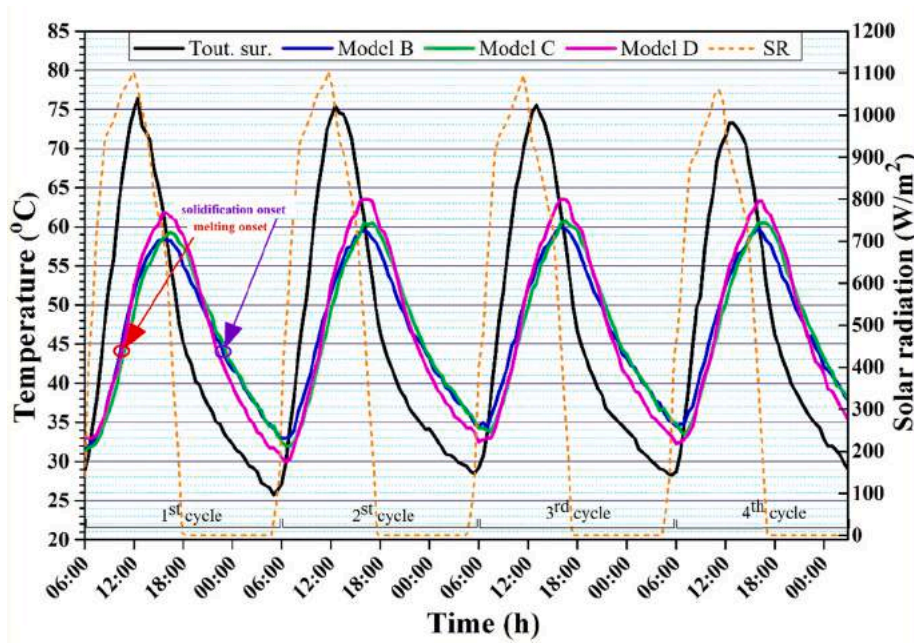
Fig. 10. ATFR for Case I and Case II.

Fig. 11. PCM temperature curves (Case II).

decreased as T_o decrease in the second half of the day cycle. This is because of low ambient temperature during late afternoon and evening, which release the heat from the PCM layer close to the finishing layer more than in other positions. Nevertheless, the PCM temperature of Model B shows better performance during the solidification phase because the heat stored by the PCM during the day was released towards the outside low temperature. Model D showed a worse thermal performance during the melting phase compared with other PCM models. During the evening period and early morning of the following cycle, the PCM temperature in this model was the closest to T_o, indicating the lack of PCM storage capacity. Following the above analysis, we can emphasise that roof layers' thermal resistance (i.e., Isogam and concrete in the present study) reduces the heat charged into each model's PCM layer

and ultimately affects its melting process. Therefore, the heat passes through the roof elements, should be high enough to utilise PCM's storage capacity, as proved in Model A.

Decrement factor (DF)

Decrement factor is another important indicator used to evaluate the decrement of peak temperature in each model considering the surface temperature. It can be defined as the cyclic temperature reduction in the roof's inside surface temperature compared to the outside surface temperature. Therefore, it can be calculated according to Eq. (5), as follows [37]:

$$DF = \frac{T_{i,max} - T_{i,min}}{T_{o,max} - T_{o,min}} \qquad (5)$$

where $T_{i,max}$, $T_{i,min}$, $T_{o,max}$ and $T_{o,min}$ are the minimum and maximum temperatures of the inside and outside surfaces of the roof (°C), respectively. In this regard, the lowest DF value means lower cyclic fluctuation of the inside temperature during the day-cycle as an advantage of PCM layer incorporation. It is worth mentioning that DF's value is important as it influences the mean radiant temperature and operative temperatures of a room and, thus, the thermal comfort. Fig. 12 shows the DF of each model in both cases.

As shown in the figure and compared with Model A, Model B has the best DF, which indicate the utilisation of PCM storage capacity to moderate the changeable inside surface temperature during the day and night. Model C also showed good behaviour of DF compared with Model D, which was the worst. It is also noted that Model B and Model C have better DF under higher temperatures (i.e., Case II) which point out the better implementation of PCM layers at outside and middle positions under high solar radiation locations. The DF obtained in Case I was 0.5–0.58, 0.51–0.58, 0.54–0.68 for Model B, Model C and Model D compared with 0.76–0.81 for Model A. Likewise, the DF for Model B, Model C, Model D were respectively in the range 0.44–0.49, 0.46–0.52, and 0.57–0.63 against 0.79–0.86 for Model A in Case II.

Time lag (TL)

TL is a convincing way to differentiate among the best position of PCM models. It can be determined as the period between the time at maximum inside surface temperature ($T_{i,max}$) and the time at maximum outside surface temperature ($T_{o,max}$), according to Eq. (6) [38], as follows:

$$TL = \tau_{T_{i,max}} - \tau_{T_{o,max}} \qquad (6)$$

where $\tau_{Ti,max}$ and $\tau_{To,max}$ are respectively the time at maximum inside and outside surface temperatures of the roof. This indicator designates the period of shifting peak load to off-load, which determines the reliance on air-conditioning systems. Fig. 13 shows the comparative period at which the TL was achieved in Case I and Case II.

Fig. 12 obviously showed that Model B and Model C have the best TL compared with Model A. In Case I, TL of Model B, Model C, Model D was

ranging from (90–150 min), (80–150 min), and (80–90 min), respectively, more than Model A. Besides, the TL of these models was ranging from (140–180 min), (140–170 min) and (110–140 min) in Case II. TL was higher in Case II than Case I, and the reason is that under high T_o the PCM is activated and stored more heat in all PCM models than the reference model. It means that the heat passed through the envelope of Model A faster than PCM models that utilised the PCM's storage capacity. Whereas, models in Case I were subjected to lower T_o, and only little amount of heat was stored in the PCM models due to the high melting temperature of PCM compared with the passed heat in this case and considering the thermal resistance of roof layers.

Both DF and TL are intrinsic indicators in the building envelope studies as they identify the heat stored in the envelope and influence the required hours for employing the cooling systems [39]. TL could be calculated twice for peaks during the day-cycle, as shown in Fig. 14. It is clear from the figure that the TL resulting from the shifting of high solar radiation during the day is more significant than that at the end of the day cycle. It emphasises the PCM layer's role to enhance the thermal mass of PCM roofs compared with the conventional roof during peak hours.

Heat flux reduction (HFR)

In the current work, we can consider only the conductive heat flux ($Q_{cond.}$) and ignoring the convective heat flux effect on both sides of the composite roof models as they exposed to the same inside and outside air films. $Q_{cond.}$ can be calculated by Fourier's formula for the composite roof, which is simplified for steady-state, one-dimensional conductive heat flux according to Eq. (7), as follows [40]:

$$Q_{cond.} = \frac{[T_o - T_i]}{\sum_1^n \frac{L}{kA}} \qquad (7)$$

where n is the number of layers (3 layers for Model A, 4 layers for Model B, Model C and Model D including PCM layer). L is the thickness of each layer (m), and k is the thermal conductivity of layers (W/m.K) in which k for the PCM layer taken for the paraffin alone neglecting that of encapsulation panel to simplify the calculations. A is the roof cross-section area (m^2).

Consequently, the reduction of heat flux of PCM models compared with the reference model can be calculated by Eq. (8), as follows:
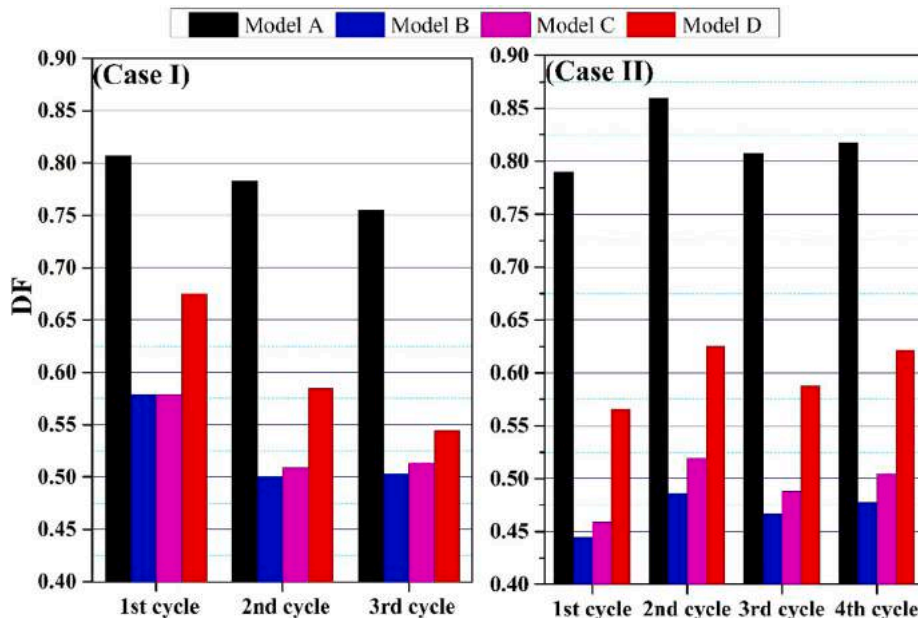
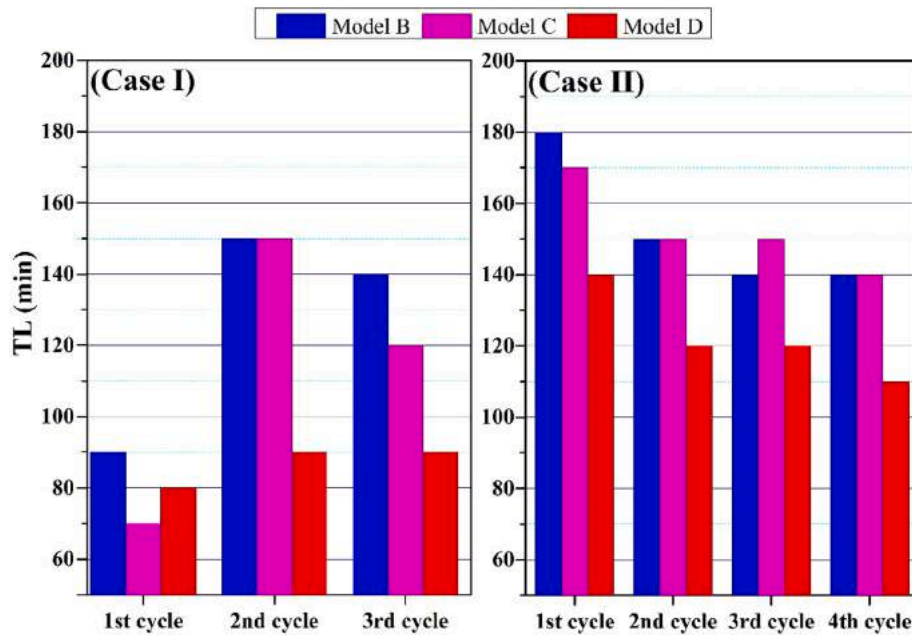

Fig. 12. DF for Case I and Case II.

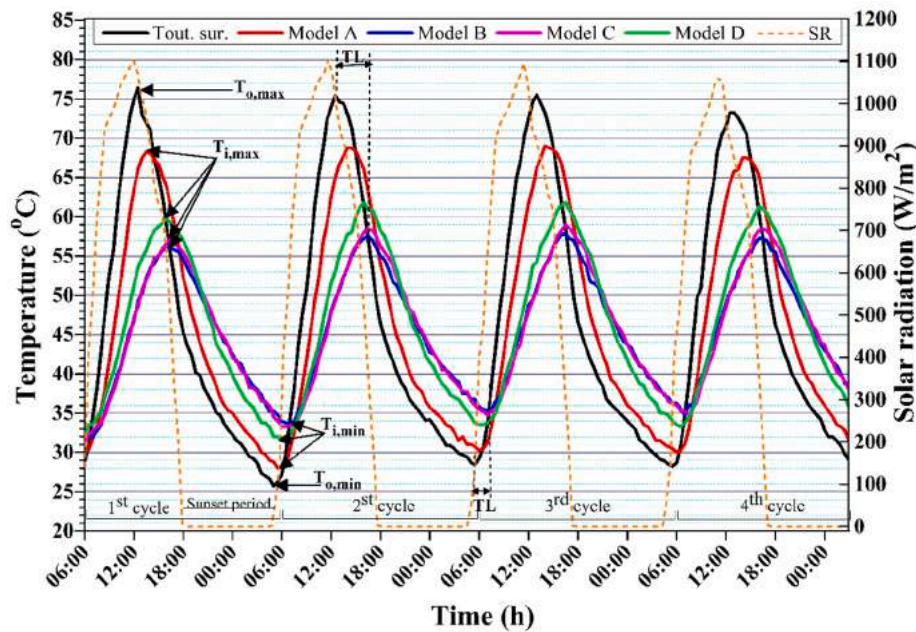**Fig. 13.** TL for Case I and Case II (based on 10 min time step measurements).

Fig. 14. Internal surface temperatures for models (Case II).

$$HFR = \frac{Q_{ref.Model} - Q_{PCMModel}}{Q_{ref.Model}} \times 100\% \qquad (8)$$

Fig. 15 shows the HFR percentage of PCM models in each case at maximum T_o and T_i in each day-cycle concerning that obtained by the referenced model.

As expected, all PCM models indicated lower heat flux than the model without PCM due to PCM incorporation. Compared with Model A, Model B showed a higher reduction of conductive heat flux followed by Model C and then, Model D. The highest HFR of Model B in Case I was achieved as 49.9% in the first cycle, whereas it was 64.6% in the fourth cycle of Case II. The HFR in Model B, Model C, Model D was ranging from 24.4 to 49.9%, 13.5–41.7%, and 7.8–29.3% in Case I. Whereas, it was ranging from 47.9 to 64.6%, 38.8–51.8%, and 20.7–25.1%,

respectively for Model B, Model C, Model D in Case II. In general, the HFR of Case II cycles was higher than that of Case I cycles. Hence, it can be concluded that the PCM layer's outer position is significantly reduced the heat flux, especially for high melting temperature PCMs [41].

Conclusions

This work aims to identify the optimal position of a macro-encapsulated PCM layer incorporated non-conditioned composite roof at different positions under hot climate conditions. Three different positions are studied, namely between the roofing layer and main roof layer, at the middle of the roof main layer, and between the roof main layer and the cladding layer. The PCM layer effect at these positions was
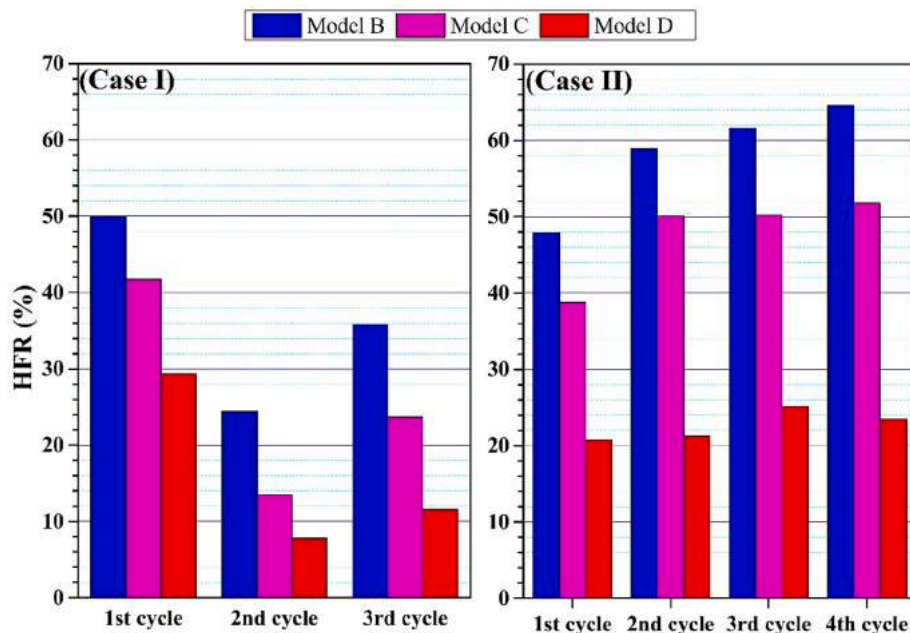
Fig. 15. HFR for Case I and Case II.

compared with a reference roof without PCM in terms of a set of indicators based on room and inside roof surface temperatures against average outside surface temperature. According to the obtained results, positioning the PCM layer between the roofing layer and the main roof layer showed the best thermal performance, especially during high solar radiation days. Although this work deals with small case rooms, the same thermal performance of PCM performance is expected for a bigger scale considering high outside temperature and non-conditioned cases. Several conclusions can be drawn from the results, as follows,

- Room temperature can be shaved remarkably by incorporating the PCM layer at all positions thanks to its thermal storage potential. The PCM position close to the outside envelope (i.e., Model B) was reached a maximum reduction of room temperature by up to 9 °C.
- PCM of high melting temperature works actively at higher outside temperatures, and its thermal storage can be utilised efficiently.
- Positioning the PCM layer close to the interior environment shows the worst thermal behaviour for non-conditioned roofs than other positions close to the exterior environment.
- Generally, all calculated indicators (i.e., room maximum temperature reduction, average maximum temperature reduction, decrement factor, time lag and heat flux reduction) showed that the PCM layer's best thermal behaviour was obtained for Model B.
- Positioning the PCM in the middle of the roof main layer (Model C) also have good thermal behaviour compared with the interior position (i.e., Model D). However, the installation at this position may influence the roof's mechanical strength as it should be involved in the main roof layer during installation.

Declaration of Competing Interest

The authors declare that they have no known competing financial interests or personal relationships that could have appeared to influence the work reported in this paper.

Acknowledgement

References

[1] International Energy Agency, UN Environment Programme. 2019 global status report for buildings and construction: Towards a zero-emission, efficient and resilient buildings and construction sector. 2019. https://webstore.iea.org/2019-global-status-report-for-buildings-and-construction. (Accessed 15 February 2021).

[2] United Nations Environment Programme. Global Status Report 2017: Towards a zero-emission, efficient, and resilient buildings and construction sector. 2017. https://www.worldgbc.org/sites/default/files/UNEP%20188_GABC_en%20%28web%29.pdf. (Accessed 15 February 2021).

[3] Al-Yasiri Q, Szabó M. Incorporation of phase change materials into building envelope for thermal comfort and energy saving: A comprehensive analysis. J Build Eng 2021;36:102122. https://doi.org/https://doi.org/10.1016/j.jobe.2020.102122.

[4] Jelle BP, Kalnæs SE. Phase Change Materials for Application in Energy-Efficient Buildings. Cost-Effective Energy Effic. Build. Retrofit. Mater. Technol. Optim. Case Stud., Elsevier Ltd 2017:57–118. https://doi.org/10.1016/B978-0-08-101128-7.00003-4.

[5] Tunçbilek E, Arıcı M, Bouadila S, Wonorahardjo S. Seasonal and annual performance analysis of PCM-integrated building brick under the climatic conditions of Marmara region. J Therm Anal Calorim 2020;141(1):613–24. https://doi.org/10.1007/s10973-020-09320-8.

[6] Jurčević M, Nižetić S, Arıcı M, Ocłoń P. Comprehensive analysis of preparation strategies for phase change nanocomposites and nanofluids with brief overview of safety equipment. J Clean Prod 2020;274:122963. https://doi.org/10.1016/j.jclepro.2020.122963.

[7] Jin X, Medina MA, Zhang X. Numerical analysis for the optimal location of a thin PCM layer in frame walls. Appl Therm Eng 2016;103:1057–63. https://doi.org/10.1016/j.applthermaleng.2016.04.056.

[8] Berardi U, Gallardo AA. Properties of concretes enhanced with phase change materials for building applications. Energy Build 2019;199:402–14. https://doi.org/10.1016/j.enbuild.2019.07.014.

[9] Lagou A, Kylili A, Šadauskienė J, Fokaides PA. Numerical investigation of phase change materials (PCM) optimal melting properties and position in building elements under diverse conditions. Constr Build Mater 2019;225:452–64. https://doi.org/10.1016/j.conbuildmat.2019.07.199.

[10] Hu J, Yu X (Bill). Adaptive building roof by coupling thermochromic material and phase change material: Energy performance under different climate conditions. Constr Build Mater 2020;262:120481. https://doi.org/10.1016/j.conbuildmat.2020.120481.

[11] Hagenau Morten, Jradi Muhyiddine. Dynamic modeling and performance evaluation of building envelope enhanced with phase change material under Danish conditions. J Energy Storage 2020;30:101536. https://doi.org/10.1016/j.est.2020.101536.

[12] Tunçbilek Ekrem, Arıcı Müslüm, Krajčík Michal, Nižetić Sandro, Karabay Hasan. Thermal performance based optimization of an office wall containing PCM under intermittent cooling operation. Appl Therm Eng 2020;179:115750. https://doi.org/10.1016/j.applthermaleng.2020.115750.

[13] Fateh A, Borelli D, Devia F, Weinläder H. Summer thermal performances of PCM-integrated insulation layers for light-weight building walls: Effect of orientation and melting point temperature. Therm Sci Eng Prog 2018;6:361–9. https://doi.org/10.1016/j.tsep.2017.12.012.

[14] Triano-Juárez J, Macias-Melo EV, Hernández-Pérez I, Aguilar-Castro KM, Xamán J. Thermal behavior of a phase change material in a building roof with and without reflective coating in a warm humid zone. J Build Eng 2020;32:101648. https://doi.org/10.1016/j.jobe.2020.101648.

[15] Soleimani Dashtaki A, Ahmadi Nadooshan A, Abedi A. The Effect of Type and Location of a Phase Change Material (PCM) Layer in a Building Wall on Energy Consumption using Numerical Simulation. ADMT J 2019;12:33–46.

[16] Arıcı Müslüm, Bilgin Feyza, Nižetić Sandro, Karabay Hasan. PCM integrated to external building walls: An optimization study on maximum activation of latent heat. Appl Therm Eng 2020;165:114560. https://doi.org/10.1016/j.applthermaleng.2019.114560.

[17] Saafi K, Daouas N. Energy and cost efficiency of phase change materials integrated in building envelopes under Tunisia Mediterranean climate. Energy 2019;187: 115987. https://doi.org/https://doi.org/10.1016/j.energy.2019.115987.

[18] Li ZX, Al-Rashed AAAA, Rostamzadeh M, Kalbasi R, Shahsavar A, Afrand M. Heat transfer reduction in buildings by embedding phase change material in multi-layer walls: Effects of repositioning, thermophysical properties and thickness of PCM. Energy Convers Manag 2019;195:43–56. https://doi.org/10.1016/j.enconman.2019.04.075.

[19] Heim Dariusz, Wieprzkowicz Anna. Positioning of an isothermal heat storage layer in a building wall exposed to the external environment. J Build Perform Simul 2016;9(5):542–54. https://doi.org/10.1080/19401493.2015.1126649.

[20] Yu Jinghua, Yang Qingchen, Ye Hong, Luo Yongqiang, Huang Junchao, Xu Xinhua, et al. Thermal performance evaluation and optimal design of building roof with outer-layer shape-stabilized PCM. Renew Energy 2020;145:2538–49. https://doi.org/10.1016/j.renene.2019.08.026.

[21] Al-Yasiri Qudama, Al-Furaiji Mushtaq A, Alshara Ahmed K. Comparative study of building envelope cooling loads in Al-Amarah city. Iraq. J Eng Technol Sci 2019;51 (5):632. https://doi.org/10.5614/j.eng.technol.sci.2019.51.510.5614/j.eng.technol.sci.2019.51.5.3.

[22] Resan SF, Chassib SM, Zemam SK, Madhi MJ. New approach of concrete tensile strength test. Case Stud Constr Mater 2020;12:1–13. https://doi.org/10.1016/j.cscm.2020.e00347.

[23] Reza Vakhshouri A. Paraffin as Phase Change Material. In: Soliman FS, editor. Paraffin - an Overv., " IntechOpen"; 2019. https://doi.org/DOI: 10.5772/intechopen.90487.

[24] Hasan MI, Basher HO, Shdhan AO. Experimental investigation of phase change materials for insulation of residential buildings. Sustain Cities Soc 2018;36:42–58. https://doi.org/10.1016/j.scs.2017.10.009.

[25] Chaichan MT, Hussein RM, Jawad AM. Thermal Conductivity Enhancement of Iraqi Origin Paraffin Wax by Nano-Alumina. Al-Khwarizmi Eng J 2017;13:83–90. https://doi.org/10.22153/kej.2017.02.003.

[26] Akeiber HJ, Wahid MA, Hussen HM, Mohammad AT. A newly composed paraffin encapsulated prototype roof structure for efficient thermal management in hot climate. Energy 2016;104:99–106. https://doi.org/10.1016/j.energy.2016.03.131.

[27] Chaichan MT, Al-Hamdani AH, Kasem AM. Enhancing a Trombe wall charging and discharg- ing processes by adding nano-Al$_2$O$_3$ to phase change materials. Int J Sci Eng Res 2016;7:736–41.

[28] Rathore PKS, Shukla SK. Potential of macroencapsulated pcm for thermal energy storage in buildings: A comprehensive review. Constr Build Mater 2019;225: 723–44. https://doi.org/10.1016/j.conbuildmat.2019.07.221.

[29] Al-Yasiri Q, Szabó M. Influential aspects on melting and solidification of PCM energy storage containers in building envelope applications. Int J Green Energy 2021. https://doi.org/https://doi.org/10.1080/15435075.2021.1890082. (in press).

[30] Ostrý M, Bantová S, Struhala K. Compatibility of Phase Change Materials and Metals: Experimental Evaluation Based on the Corrosion Rate. Molecules 2020;25: 2823. https://doi.org/10.3390/molecules25122823.

[31] Ardunic. Ardunic Sinaa, Baghdad, Iraq n.d. https://ardunic.com/auth.

[32] PVGIS: European Comunities 2021. https://ec.europa.eu/jrc/en/pvgis.

[33] Kenzhekhanov S, Memon SA, Adilkhanova I. Quantitative evaluation of thermal performance and energy saving potential of the building integrated with PCM in a subarctic climate. Energy 2020;192:116607. https://doi.org/https://doi.org/10.1016/j.energy.2019.116607.

[34] Saxena R, Rakshit D, Kaushik SC. Experimental assessment of Phase Change Material (PCM) embedded bricks for passive conditioning in buildings. Renew Energy 2020;149:587–99. https://doi.org/10.1016/j.renene.2019.12.081.

[35] Castell A, Martorell I, Medrano M, Pérez G, Cabeza LF. Experimental study of using PCM in brick constructive solutions for passive cooling. Energy Build 2010;42(4): 534–40. https://doi.org/10.1016/j.enbuild.2009.10.022.

[36] Alam M, Jamil H, Sanjayan J, Wilson J. Energy saving potential of phase change materials in major Australian cities. Energy Build 2014;78:192–201. https://doi.org/10.1016/j.enbuild.2014.04.027.

[37] Sun C, Shu S, Ding G, Zhang X, Hu X. Investigation of time lags and decrement factors for different building outside temperatures. Energy Build 2013;61:1–7. https://doi.org/10.1016/j.enbuild.2013.02.003.

[38] Thongtha A, Khongthon A, Boonsri T, Hoy-Yen C. Thermal effectiveness enhancement of autoclaved aerated concrete wall with PCM-contained conical holes to reduce the cooling load. Materials (Basel) 2019;12:2170. https://doi.org/10.3390/ma12132170.

[39] Toure Pape Moussa, Dieye Younouss, Gueye Prince Momar, Sambou Vincent, Bodian Seckou, Tiguampo Sumailla. Experimental determination of time lag and decrement factor. Case Stud Constr Mater 2019;11:e00298. https://doi.org/10.1016/j.cscm.2019.e00298.

[40] Holman JP. Heat transfer. 10th ed. MC GRAW HILL INDIA; 2011.

[41] Al-Absi ZA, Isa MHM, Ismail M. Phase change materials (PCMs) and their optimum position in building walls. Sustain 2020;12:1294. https://doi.org/10.3390/su12041294.